Available online at www.sciencedirect.com
SCIENCE DIRECT®
Experimental Parasitology 111 (2005) 105–114
Experimental Parasitology
www.elsevier.com/locate/yexpr

Plasmodium falciparum: Stage specific effects of a selective inhibitor of lactate dehydrogenase

Livia Vivas [a,*], Anna Easton [a], Howard Kendrick [a], Angus Cameron [b], Jose-Luis Lavandera [c], David Barros [c], Federico Gomez de las Heras [c], R. Leo Brady [b], Simon L. Croft [a]

[a] *Department of Infectious and Tropical Diseases, London School of Hygiene and Tropical Medicine, London, WC1E 7HT, UK*
[b] *Department of Biochemistry, University of Bristol, Bristol, BS8 1TD, UK*
[c] *GlaxoSmithKline, Parque Tecnologico de Madrid, Severo Ochoa, 2, 28760-Tres Cantos, Madrid, Spain*

Received 4 March 2005; received in revised form 9 June 2005; accepted 29 June 2005
Available online 11 August 2005

Abstract

Plasmodium falciparum lactate dehydrogenase (*Pf*LDH) is essential for ATP generation. Based on structural differences within the active site between *P. falciparum* and human LDH, we have identified a series of heterocyclic azole-based inhibitors that selectively bind within the *Pf*LDH but not the human LDH (hLDH) active site and showed anti-malarial activity in vitro and in vivo. Here we expand on an azole, OXD1, from this series and found that the anti-*P. falciparum* activity was retained against a panel of strains independently of their anti-malarial drug sensitivity profile. Trophozoites had relatively higher *Pf*LDH enzyme activity and *Pf*LDH-RNA expression levels than rings and were the most susceptible stages to OXD1 exposure. This is probably linked to their increased energy requirements and consistent with glycolysis being an essential metabolic pathway for parasite survival within the erythrocyte. Further structural elaboration of these azoles could lead to the identification of compounds that target *P. falciparum* through such a novel mechanism and with more potent anti-malarial activity.

Index descriptors and abbreviations: PfLDH, *Plasmodium falciparum* lactate dehydrogenase; hLDH, human lactate dehydrogenase; DNA, deoxyribonucleic acid; RNA, ribonucleic acid; ATP, adenosine triphosphate; NAD, nicotinamide adenine dinucleotide; PBS, phosphate buffer saline; APAD, 3-acetyl pyridine adenine dinucleotide; RBC, red blood cells; URBC, uninfected red blood cells; IRBC, infected red blood cells; PCR, polymerase chain reaction; IC_{50}, fifty percent inhibitory concentration; GAPDH, glyceraldehyde-3-phosphate dehydrogenase

Keywords: Protozoa; *Plasmodium falciparum*; Lactate dehydrogenase; Inhibition; Intraerythrocytic cycle; Stage specificity

1. Introduction

Malaria remains a major threat to public health worldwide. It is estimated that 1–2 million children die each year mostly in Sub-Saharan Africa from the severe complications of *Plasmodiun falciparum* malaria (Guerin et al., 2002) Attempts to reduce the rates of morbidity and mortality have been hampered by the increasingly limited efficacy of current anti-malarial drugs to which *P. falciparum* has developed resistance (Olliaro and Taylor, 2003). Thus, renewed efforts are required to develop novel and affordable anti-malarials to overcome the detrimental effects of drug resistance, particularly in developing countries (Ridley, 2003).

Glycolysis represents the main source of ATP generation during the asexual intraerythrocytic cycle (Lang-Unnasch and Murphy, 1998). Glucose uptake is between 30 and 100 times higher than that of the uninfected

* Corresponding author. Fax: +44 020 76374314.
E-mail address: livia.vivas@lshtm.ac.uk (L. Vivas).

0014-4894/$ - see front matter © 2005 Elsevier Inc. All rights reserved.
doi:10.1016/j.exppara.2005.06.007

erythrocyte (Jensen et al., 1983), almost all of which is converted to lactate (Homewood and Neame, 1983). The increased metabolic activity of the parasite during this period is reflected in the high levels and activity of glycolytic enzymes compared to those of the erythrocyte (Roth, 1990). As there appears to be no functioning citric acid cycle in the erythrocytic stages of the parasite life cycle, the NADH required for glycolysis to proceed is regenerated from NAD^+ via the conversion of pyruvate (the product of glycolysis) to lactate. This reaction is catalyzed by lactate dehydrogenase (LDH), the final enzyme of the glycolytic pathway in *Plasmodium*. Crystallographic analysis of *Pf*LDH (Dunn et al., 1996) revealed an enlarged active site cavity in comparison to mammalian forms of the enzyme, suggesting that highly selective inhibitors could be designed for the parasite enzyme. In contrast to compounds such as gossypol derivatives that inhibit *Pf*LDH by binding to the co-factor site (Gomez et al., 1997), we have identified a series of heterocyclic azole-based compounds that selectively inhibit *Pf*LDH at sub-micromolar concentrations, typically at concentrations about 100-fold lower than those required to inhibit human LDH (Cameron et al., 2004). Crystallographic analysis of enzyme–azole complexes showed that this class of compounds bind to the substrate binding site and are competitive with lactate. These compounds showed low micromolar activity against drug sensitive 3D7 and drug resistant K1 strains of *P. falciparum* in vitro, low cytotoxicity in mammalian cells and were effective in suppressing parasitemia during infection with the rodent malaria parasite *P. berghei* (Cameron et al., 2004). In this paper, we describe the *P. falciparum* stage-specific effects of the most active and *Pf*LDH-specific compound of this series, the oxadiazole 4-hydroxy-1,2,5-oxadiazole-3-carboxylic acid (OXD1), the correlation between inhibition of *Pf*LDH enzyme activity by OXD1 and *Pf*LDH RNA expression levels, and in addition, attempt to establish if the parasites retain their growth potential after OXD1 exposure during the intraerythrocytic development of the asexual stages. These data support the principle that specific inhibitors that bind into the active site of *Pf*LDH can form viable and effective anti-malarial compounds.

2. Materials and methods

2.1. Plasmodium falciparum in vitro culture and synchronization

All parasite clones, isolates and strains were acquired from MR4 (Malaria Research and Reference Reagent Resource Center, Manassas, Virginia, USA). Strains/isolates used in this study were: the drug sensitive 3D7 clone of the NF54 isolate (unknown origin); the drug sensitive strains FCR-8 (The Gambia) and FCC2 (China); the chloroquine, pyrimethamine and cycloguanil resistant K1 strain (Thailand); the chloroquine and pyrimethamine resistant FCR3 strain (The Gambia); the chloroquine resistant FCB strain (Colombia) and the chloroquine, pyrimethamine, cycloguanil, and mefloquine resistant isolate Tm90C2A (Thailand). In vitro culture of *P. falciparum* was carried out following standard methods (Trager and Jensen, 1976) with modifications as described (Cameron et al., 2004). Synchronization of parasite growth was achieved by Percoll and sorbitol treatment as described previously (Fleck et al., 2003).

2.2. In vitro parasite growth inhibition assays

The method used to assess parasite growth was based on the [^{3}H]hypoxanthine incorporation assay (Desjardins et al., 1979) with modifications including the use of Albumax instead of 10% human plasma to supplement the culture medium. Due to the absence of hypoxanthine in Albumax-based medium, addition of unlabelled hypoxanthine was found to be essential for optimal parasite growth and [^{3}H]hypoxanthine incorporation in asynchronous cultures during the 48 h growth-assay period. Addition of unlabelled hypoxanthine at a concentration 15 μM at the beginning of the assay, ensured that [^{3}H]hypoxanthine (0.048 μM, specific activity 17.40 Ci/mmol) uptake was linear up to 1% parasitemia, thus enabling detection of small reductions in the parasitemia (within the range of 0.1–1%). Stock drug solutions were dissolved in 100% dimethyl sulfoxide (Sigma, Dorset, UK) and 50 μl of a 2-fold dilution series (192, 96, 48, 24, 12, 6, and 3 μM) of the drugs prepared in assay medium (RPMI 1640 supplemented with 0.5% Albumax II (Invitrogen), 0.2% w/v glucose, 0.03% L-glutamine, and 15 μM hypoxanthine) added to each well of 96-well plates in triplicate. Fifty microlitres of asynchronous (65–75% ring stage) *P. falciparum* culture (0.5% parasitemia) or uninfected erythrocytes were added to each well reaching a final volume of 100 μl per well, a final hematocrit of 2.5% and final dimethyl sulfoxide concentrations $\leqslant$0.01%. Plates were incubated at 37 °C in 5% CO_2, and 95% air mixture for 24 h, at which point 20 μl (0.1 μCi/well) of [^{3}H]hypoxanthine (Perkin-Elmer, Hounslow, UK) was added to each well. The addition of 0.1 μCi per well instead of 0.5 μCi as described by Desjardins et al. was found to provide a satisfactory range of CPM between the maximum incorporation in untreated cultures and that of uninfected red cells. Plates were mixed for 1 min using a plate shaker and returned to the incubator. After an additional 24 h incubation period, the experiment was terminated by placing the plates in a −80 °C freezer. Plates were thawed and harvested onto glass fibre filter mats using a 96-well cell harvester (Harvester 96, Tomtec, Oxon, UK) and left to dry. After the addition of MeltiLex solid scintillant (Perkin–Elmer,

Hounslow, UK) the incorporated radioactivity was counted using a Wallac 1450 Betalux scintillation counter (Wallac). All assays included chloroquine diphosphate as a standard and control wells with untreated infected and uninfected erythrocytes. Data acquired by the Wallac BetaLux scintillation counter were exported into a MICROSOFT EXCEL spreadsheet (Microsoft), and the IC_{50}/IC_{90} values of each drug were calculated by using XLFit (ID Business Solutions, UK) line fitting software.

2.3. In vitro cytotoxicity assay

The AlamarBlue (Accumed International, USA) method was used to assess cytotoxicity to KB cells as previously described (Cameron et al., 2004). Briefly, microtiter plates were seeded at a density of 4×10^4 KB cells/ml in RPMI 1640 culture medium supplemented with 10% heat-inactivated fetal calf serum (complete medium) (Seralab). Plates were incubated at 37 °C, 5% CO_2, 95% air mixture for 24 h followed by compound addition to triplicate wells in a dilution series in complete medium. The positive control drug was podophyllotoxin (Sigma). Plates were incubated for a further 72 h followed by the addition of 10 μl of Alamar-Blue (AccuMed International) to each well and incubation for 2–4 h at 37 °C, 5% CO_2, 95% air mixture. Fluorescence emission at 585 nm was measured in a SPECTRAMAX GEMINI plate reader (Molecular Devices) after excitation at 530 nm. ED_{50} values were calculated using XLFit (ID Business Solutions, UK) line fitting software.

2.4. Flow cytometry

Synchronized trophozoite cultures were incubated with different dilutions of OXD1 as described for the in vitro drug inhibition assay. Following a 48 h-incubation period, dihydroethidine (Polysciences, PA, USA) was added at 10 μg/ml in PBS to each well and incubated for 20 min at 37 °C in the dark. IRBC were washed with PBS once and then fixed with 1% paraformaldehyde in PBS. URBC were included as controls. The intensity of fluorescence emitted in the FL2 channel was analyzed by flow cytometry on a Becton–Dickinson FACScan. IC_{50} values were calculated using Microsoft (Microsoft) *XLFit* (IDBS, UK) line fitting software.

2.5. PfLDH enzyme activity

Highly synchronized cultures containing known numbers of IRBC or URBC were lysed with saponin (0.05% in PBS) and directly assayed for *Pf*LDH activity. The assay is based on the reduction of 3-acetyl pyridine adenine dinucleotide (APAD) to APADH, a NAD^+ derivative that is specific for *Pf*LDH, which allows the distinction of *Pf*LDH from that of the host RBC (Makler et al., 1993). A standard curve was constructed using recombinant *Pf*LDH that had previously been shown to be kinetically indistinguishable from the native form (Shoemaker, PhD Thesis, University of Bristol, 2001) and the levels of *Pf*LDH determined were expressed as molar concentrations inside IRBC. The formation of APADH was measured at 655 nm in a SPECTRAMAX GEMINI plate reader (Molecular Devices, USA) using a linked assay containing 2 mM phenazine ethosulfate, 1 mg/ml nitroblue tetrazolium, 12.5 mM lactate, and 50 mM $APAD^+$ in PET buffer [50 mM Tris–HCl (tris(hydroxymethyl)aminomethane hydrochloride), 50 mM KCl, 1 mM EDTA (ethylenediaminetetraacetic acid), and 3% (w/v) PEG (polyethyleneglycol 6000), pH 7.5 (All Sigma).

2.6. Stage-specific PfLDH gene expression by quantitative real-time PCR

Aliquots of parasitized erythrocytes taken every 6 h from highly synchronized *P. falciparum* 3D7 cultures were lysed with saponin (0.05% in PBS) and washed five times with ice-cold PBS. RNA extraction was performed using the Qiagen RNeasy Kit and treated with DNAse (Qiagen, Crawley, UK) to remove any contaminating genomic DNA (1 μl from each sample was subjected to PCR as described below to detect DNA contamination). Isolated RNA from *P. falciparum* 3D7 was reverse transcribed to obtain cDNA using the OmniScript Reverse Transcriptase Kit (Qiagen) and the specific forward 3′-C CACCAATTTCAATCATAATCTT and reverse primer 5′-GGCTGGAGCAGATGTAGTAATAG (Genset, Evry, France) designed to amplify a 149 bp region of the *Pf*LDH gene (GenBank Accession No. AF25129). The 18s rRNA internal control (Blair et al., 2002) was amplified using forward P.fal 18s F 5′-GCTGACTACGTCC CTGCCC, and reverse primer P.fal 18s R 5′-ACAATT CATCATATCTTTCAATCGGTA. The PicoGreen dsDNA Quantitation Kit (Molecular Probes, Leiden, The Netherlands) was used for accurate quantitation of dsDNA and a standard curve constructed for each primer pair. Each PCR product was diluted from an initial concentration of 10^8 molecules/μl using a 10-fold dilution series down to 10^{-3} molecules/μl. PCR was performed as above for 50 cycles to check the PCR efficiency, standard curve quality and that no PCR products were detectable at 0, 0.1, 0.01, and 0.001 molecules/μl. cDNA synthesis was carried out prior to real-time PCR analysis and 1 μl of cDNA from each time point was used per reaction in duplicate for both LDH and 18s rRNA. Real-time PCR analysis was carried out on a ABI Prism 7700 Sequence Detector (Applied Biosystems, Warrington, UK) using the SYBR Green PCR Kit (Applied Biosystems). LDH mRNA expression was determined by the standard curve relative expression method. This was achieved by measuring the relative

quantities of the endogenous calibrator 18s rRNA to observe the expression levels of *pf*LDH. Values derived from the standard curve for 18s rRNA and *Pf*LDH were averaged for each time point and the value for *Pf*LDH was divided by the value for 18s rRNA to obtain a calibrated ratio. Each ratio was then normalized to the sample point $t=0$ to obtain relative expression levels of *Pf*LDH throughout the life cycle.

2.7. Confocal microscopy

Thin blood films were taken from cultures at ring, trophozoite and schizont stages using poly-L-lysine coated slides (BDH/Merck, Lutterworth, UK) air-dried and fixed in cold acetone for 30 min at −20 °C. Slides were allowed to dry at room temperature prior to the addition of a rabbit polyclonal serum (1:8 dilution) raised by immunization with purified recombinant *Pf*LDH protein expressed in *Escherichia coli* $CaCl_2$-competent cells. In Western blotting experiments, this anti-*Pf*LDH polyclonal serum specifically recognized the recombinant product but no reactivity was observed with the pre-immune serum (Turgut-Balik et al., 2001). After 30 min incubation in a humidity chamber at 37 °C, slides were washed three times with PBS prior to addition of a mouse monoclonal anti-rabbit IgG gamma chain specific FITC (fluorescein isothiocyanate) conjugate (Sigma) at a dilution of 1:80. Slides were placed in a humidity chamber at 37 °C for a further 30 min in the dark and then washed as above, prior to incubation for 20 min at room temperature with PBSA (1% bovine serum albumin in PBS) (All Sigma) containing RNase at 10 mg/ml and 0.1% saponin to prevent propidium iodide (PI) (Sigma) binding to RNA. One drop of Vectashield (Vector Laboratories, Peterborough, UK) containing PI was then added and a cover slip placed over the slide. Fluorescence was examined using a LSM 510 Axioplan confocal microscope (Zeiss, Germany) at 488 nm for FITC and at 543 nm for PI. Normal light images were also taken and combined with the fluorescent images to identify parasite localization within the erythrocyte and the presence of hemozoin crystals for identification of the food vacuole.

2.8. Stage specificity of OXD1

Highly synchronized ring cultures at 0.5% parasitemia and 5% hematocrit were exposed to OXD1 at 192 μM or chloroquine at 0.04 μM for 6 h during the 48 h cycle. Parasites were incubated with the compound for 6 h, washed twice and resuspended in warm RPMI 1640-Albumax medium without OXD1, prior to return to a 37 °C, 5% CO_2 incubator until completion of the cycle. Thin blood films were taken at 48 h and at different time points during incubation, fixed with 100% methanol and stained with 10% Giemsa (BDH/Merck) for microscopical examination and differential counting of rings, trophozoites, and schizonts. Alternatively, OXD1 (192 μM) or chloroquine (0.04 μM) was added at 0, 6, 12, 18, 24, 30, 36, and 42 h cultures and incubated in the presence of the compounds until completion of the 48 h cycle. Thin blood films were taken at 48 h and the proportion of rings indicative of reinvasion and cycle progression quantified by microscopy. Parasites showing pycnotic morphology, indicative of cell death, were considered non-viable.

2.9. Potential for growth over subsequent cycles

Parasites at the ring or trophozoite stage (0.5% parasitemia and 2.5% hematocrit) were exposed to OXD1 for 48 or 96 h at 768 or 384 μM. Pyrimethamine (Sigma) at 4 or 40 μM and chloroquine diphosphate at 2 or 0.4 μM were used as controls. Following incubation, OXD1 and control drugs were removed by centrifugation and the parasites washed three times with warm RPMI 1640 before being transferred back into culture. The culture medium (RPMI-Albumax) was changed daily and parasite growth and morphology monitored by daily microscopical examination of Giemsa (BDH/Merck) stained thin blood smears for a period of 2–3 weeks. Untreated parasites were included as controls and diluted 4-fold every 48 h to prevent cultures from overgrowing. Untreated parasites had a normal growth rate, with parasitemia increasing 4- to 6-fold in each 48 h cycle.

3. Results

3.1. In vitro antimalarial activity of OXD1

We previously reported that the azole OXD1 (Fig. 1A) had anti-*P. falciparum* activity against 3D7 and K1 strains (Cameron et al., 2004). Here we have further examined this activity against another six *P. falciparum* strains in the [^{3}H]hypoxanthine assay. The IC_{50} values of OXD1 were comparable against all of the strains tested independently of their anti-malarial drug sensitivity profiles and low levels of cytotoxicity to mammalian KB cells were found (Table 1). The anti-*P. falciparum* activity was confirmed by the use of hydroethidine and morphological evaluation by microscopy using synchronized trophozoites because rings were shown not to sufficiently metabolize HE at detectable levels (not shown). Hydroethidine is readily metabolized by viable cells to ethidium bromide which then intercalates into DNA producing a red fluorescence (Wyatt et al., 1991) and has been used previously to assess inhibition of *P. falciparum* growth *in vitro* by flow cytometry (Azas et al., 2002). Flow cytometric analysis revealed that in the absence of OXD1, trophozoite-infected red blood cells were detected as a distinctive

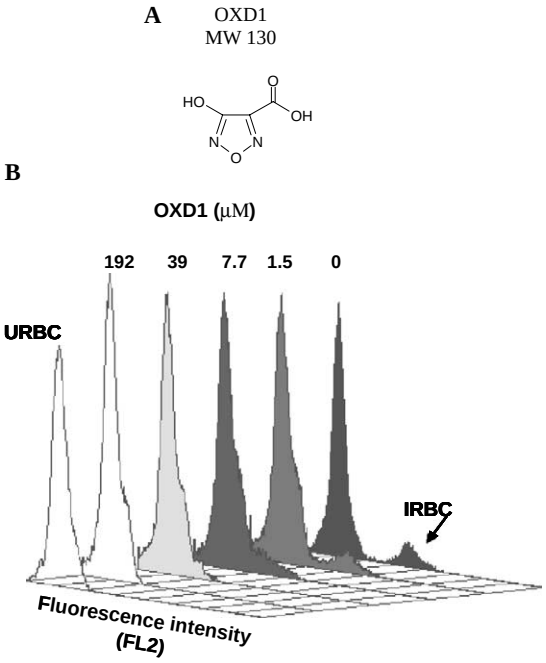

Fig. 1. (A) Chemical structure of OXD1. (B) Flow cytometric analysis of the metabolism of the vital dye hydroethidine following 48 h incubation with OXD1 at the concentrations indicated. Conversion of hydroethidine to ethidium bromide is measured in the FL2 channel. IRBC, infected red blood cells. URBC, uninfected red blood cells. The results shown are from one representative of five independent experiments.

population in the FL2 channel (Fig. 1B). A dose-dependent inhibition of hydroethidine metabolism was indicated by a reduction in the intensity of fluorescence of the IRBC population which was maximal at 192 μM OXD1, the maximum concentration used, similar to the fluorescence profile obtained from URBC which lack DNA. A comparison of the IC_{50} values obtained by the incorporation of [^{3}H]hypoxanthine, flow cytometry, and microscopic examination of thin blood films is shown in Table 2. The use of asynchronous (65–75% rings) or synchronous trophozoite cultures did not have an effect on the IC_{50} values of OXD1 determined in the [^{3}H]hypoxanthine incorporation assay. Despite incorporation of [^{3}H]hypoxanthine being totally inhibited after OXD1 192 μM exposure, morphological examination of cultures revealed 70–80% non-viable parasites as determined by the presence of pycnotic morphology indicative of cell death, but the remaining parasites looked morphologically normal and had not matured beyond the ring stage.

3.2. *Plasmodium falciparum* LDH RNA expression, enzyme activity, and intracellular localization

Lactate production has been shown to increase during the late stages of the intraerythrocytic cycle of *P. falciparum* (Vander Jagt et al., 1981) indicating high levels

Table 1
In vitro anti-malarial activity of OXD1

P. falciparum	Compound GM IC_{50} (range)				
	OXD1 ($\times 10^3$)	CQ	PYR[a]	MEF	ART
3D7	20.1 (13.6–26.1)	6.4 (2.1–16.5)	35 (28.0–72.8)	7.0 (9.6–14.9)	4.9 (3.5–9.1)
K1	19.3 (14.1–28.1)	0.25 (0.19–0.35) $\times 10^3$	11.9 (10.2–12.6) $\times 10^3$	3.3 (2.1–5.6)	3.8 (1.9–9.2)
W2	27.2 (24.3–30.3)	0.9 (0.6–1.3) $\times 10^3$	29.3 (29.0–29.6) $\times 10^3$	1.48 (1.46–1.49)	3.1 (2.6–3.7)
FCR-8	19.4 (18.8–19.9)	10.8 (10.6–11.0)	29.9 (26.0–34.4)	ND	5.0 (3.4–7.3)
FCC-2	21.9 (18.9–25.4)	13.2 (11.0–15.8)	5.4 (4.1–7.2) $\times 10^3$	ND	5.5 (3.9–7.8)
FCB	21.8 (18.2–25.8)	0.2 (0.1– 0.3) $\times 10^3$	57.4 (38.4–72.4)	0.68 (0.67–0.68)	7.5 (7.3–8.1)
FCR3	20.0 (18.7–21.5)	0.3 (0.2–0.4) $\times 10^3$	64.1 (40–120)	0.27 (0.26–1.06)	6.1 (5.2–7.3)
TM90C2A	30.0 (29.1–30.9)	0.14 (0.11–0.27) $\times 10^3$	70.1 (59.6–76.0) $\times 10^3$	15.4 (10.4–22.9)	8.9 (8.0–9.4)
KB GM CC_{50} (range)	1349.6 (1036.8–1756.7)	ND	ND	ND	ND

In vitro anti-malarial activity of OXD1 against eight *P. falciparum* strains measured by the incorporation of [^{3}H]hypoxanthine. The final row indicates cytotoxicity of OXD1 to the mammalian KB cell line measured by the Alamar blue method. CQ, chloroquine; PYR, pyrimethamine; MEF, mefloquine; ART, artesunate. ND, not determined. Results shown are the geometric mean IC_{50} values and the range in nM from 3 to 10 independent experiments. GM, geometric mean.

[a] Pyrimethamine was tested in standard assay medium containing 1 μg/ml folic acid and 1 μg/ml *para*-amino benzoic acid (pABA).

Table 2
Comparison of IC_{50} values against 3D7 obtained using three different assays to determine inhibition of *P. falciparum* growth in vitro

Compound	*P. falciparum* 3D7 GM IC_{50} (range)		
	[^{3}H]Hypoxanthine	Flow cytometry	Light microscopy
OXD1	20.1 (13.6–26.1) $\times 10^3$	20.3 (12.2–22.4) $\times 10^3$	28.3(15.8–33.9) $\times 10^3$
CQ	6.4 (2.1–16.5)	16.6 (9.7–30.9)	9.5 (3.9–23.1)

In vitro anti-malarial activity of OXD1 was determined by [^{3}H]hypoxanthine incorporation, flow cytometry using the vital dye hydroethidine, and light microscopy of Giemsa-stained thin blood films following incubation with the compound for 48 h. CQ, chloroquine. Results shown are the geometric mean IC_{50} values and the range in nM from 3 to 10 independent experiments.

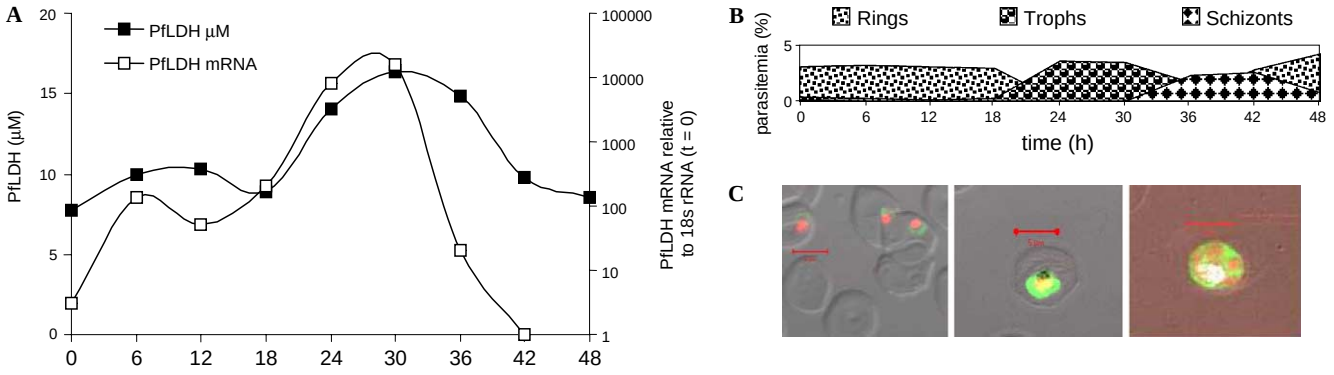

Fig. 2. *Plasmodium falciparum* 3D7 LDH RNA expression levels, enzyme activity and intracellular localization. (A) PfLDH enzyme activity, PfLDH-mRNA levels and PfLDH confocal immunofluorescence imaging during the intraerythrocytic development of the asexual forms of *P. falciparum* 3D7. (B) Cycle progression over 48 h. (C) Confocal imaging of *P. falciparum* intra-erythrocytic stages labelled with a rabbit anti-PfLDH polyclonal antibody-FITC (green) and nuclear labelling with propidium iodide (red). Note the cytoplasmic green fluorescence compatible with PfLDH intracellular cytoplasmic localization. Results are from one representative of two independent experiments. (For interpretation of the references to colour in this figure legend, the reader is referred to the web version of this paper.)

of *Pf*LDH enzyme activity. To characterize in more detail the target enzyme, levels of PfLDH RNA and enzyme activity were measured at 6 h intervals during the 48 h intra-erythrocytic cycle. The use of 18s rRNA as an internal endogenous standard was preferred because GAPDH expression could be directly associated with LDH expression (as they share the same biochemical pathway) and 18s rRNA content is proportional to the total amount of RNA present in the cell. As shown in Fig. 2A, *Pf*LDH RNA expression levels gradually increased, reaching a peak between 24 and 30 h in the intraerythrocytic cycle, and decreased to almost zero in the schizont stage. A similar profile of enzyme activity that lagged slightly behind the *Pf*LDH RNA levels was observed. The levels of *Pf*LDH RNA and enzyme activity showed a slight but non-significant reduction at 12 and 18 h, respectively, prior to the peak. The parasite cytoplasmic localization of *Pf*LDH was confirmed by confocal microscopy. Compared to the ring stages, an intense green cytoplasmic diffuse fluorescence pattern was observed in the trophozoite and schizont stages (Fig. 2C) with no fluorescence detected in the food vacuole or the nucleus suggesting accumulation in the parasite cytoplasm. No fluorescence was detected in URBC confirming parasite specific LDH reactivity of the antibody. Cycle progression is shown in Fig. 2B.

3.3. Relative sensitivity of the different asexual parasite stages

The sensitivity of the different parasite stages of the asexual cycle to OXD1 was examined by exposure to OXD1 (Fig. 3) for periods of 6 h at different time points, followed by washing and subculture in the absence of compound until completion of the 48 h cycle. Microscopical examination of blood films taken at the end of the 48 h cycle revealed that compared to

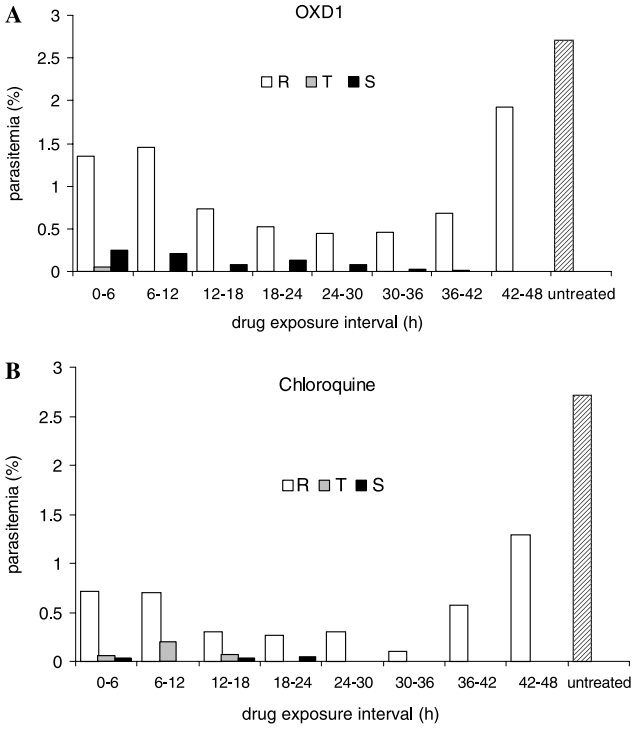

Fig. 3. Stage sensitivity of *P. falciparum* 3D7 to OXD1. Highly synchronized cultures were exposed to (A) OXD1 at 192 μM or (B) chloroquine at 0.04 μM. Cultures were exposed to OXD1 for 6 h during the 48 h-intraerythrocytic cycle (from 0–6, 6–12, 12–18, 18–24, 24–30, 30–36, 36–42, and 42–48 h), washed twice with RPMI 1640 after each interval to remove the compounds, and returned to the incubator to complete the 48 h cycle. The levels of parasitemia were determined microscopically by differential counting of viable parasites in blood films taken at 48 h. Empty bars, rings; shaded bars, trophozoites; and filled bars, schizonts. Results are from one representative of two independent experiments.

untreated cultures, in which the parasitemia exclusively consisted of new rings, exposure to OXD1 in the first 12 h of the cycle reduced the parasitemia by about 50%

and by 80–86% if exposure to OXD1 was between 18–24, 24–30, and 30–36 h. Coupled to a reduction in the levels of parasitemia, there was a delay in the progression of the cycle as a proportion of the parasite population was still at the schizont stage. This delay was more apparent when the compound was applied at the ring stage, between 0 and 12 h, but a proportion of parasites did progress to the end of the cycle and reinvaded. Reinvasion was indicated by an increase in the level of parasitemia from 0.5% (initial parasitemia) to 1.4–1.5% of rings when OXD1 was applied between 0–6 and 6–12 h and close to 2% when OXD1 was applied after 42 h.

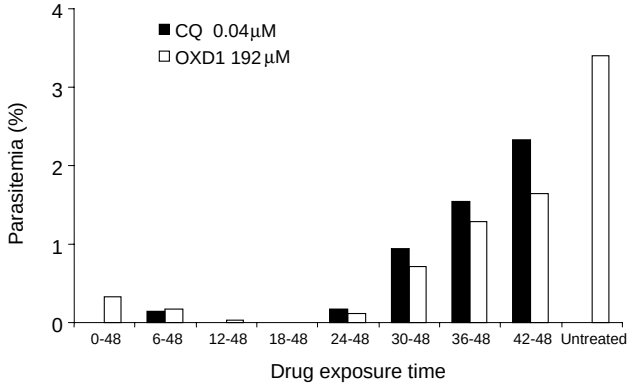

Fig. 4. Effects of the length of exposure and the time of OXD1 addition on cycle progression and reinvasion. Highly synchronous *P. falciparum* 3D7 ring-stage cultures were exposed to OXD1 (192 μM) or CQ (0.04 μM). OXD1 was added to cultures at different time points (0, 6, 12, 18, 24, 30, 36, and 42 h) and incubated with the compounds until completion of the 48 h cycle. Reinvasion was assessed from viable ring counts determined by microscopic examination of thin blood films taken at 48 h. Results are from one representative of two independent experiments. CQ, chloroquine.

To investigate in more detail the influence of the timing and length of exposure to OXD1 necessary to attain the inhibitory effect, highly synchronized ring cultures were exposed to OXD1 (192 μM) added at different times every 6 h and incubated with the compound until completion of the 48 h cycle at which point blood films were taken and examined by microscopy (Fig. 4). Quantification of the viable ring population at 48 h, revealed that the parasitemia increased from 0.5 to 3.4% in the untreated cultures, reflecting the natural progression of the cycle and reinvasion. Incubation with OXD1 from 0 to 48 h reduced the numbers of viable parasites by 80% (from 0.5 to 0.1% parasitemia at 192 μM). The remaining viable parasites were growth-arrested rings rather than newly invaded parasites because monitoring of the progression of the 48 h cycle every 6 h by microscopy did not revealed the presence of other stages (Fig. 5A). Incubation with OXD1 at 192 μM (Fig. 4) from 12 to 48 h and from 18 to 48 h appeared to completely inhibit cycle progression as no rings were observed. Addition of the compound in the last 24 h of the cycle resulted in reinvasion. These effects are shown in Fig. 5A in which, compared to the untreated controls, there was no maturation of rings when 192 μM OXD1 was added at time 0 h (early rings) and monitored by microscopy every 12 h during the 48 h cycle. Addition of OXD1 (192 μM) at 12 and 18 h and exposure until the end of the 48 h cycle, led to morphological changes suggestive of pycnosis and indicative of cell death (Fig. 5B) compared to untreated cultures, which did progress to reinvasion. No morphological alterations were observed in URBC. Taken together, these results indicate that the trophozoites (12–18 h) had an increased susceptibility to *Pf*LDH inhibition.

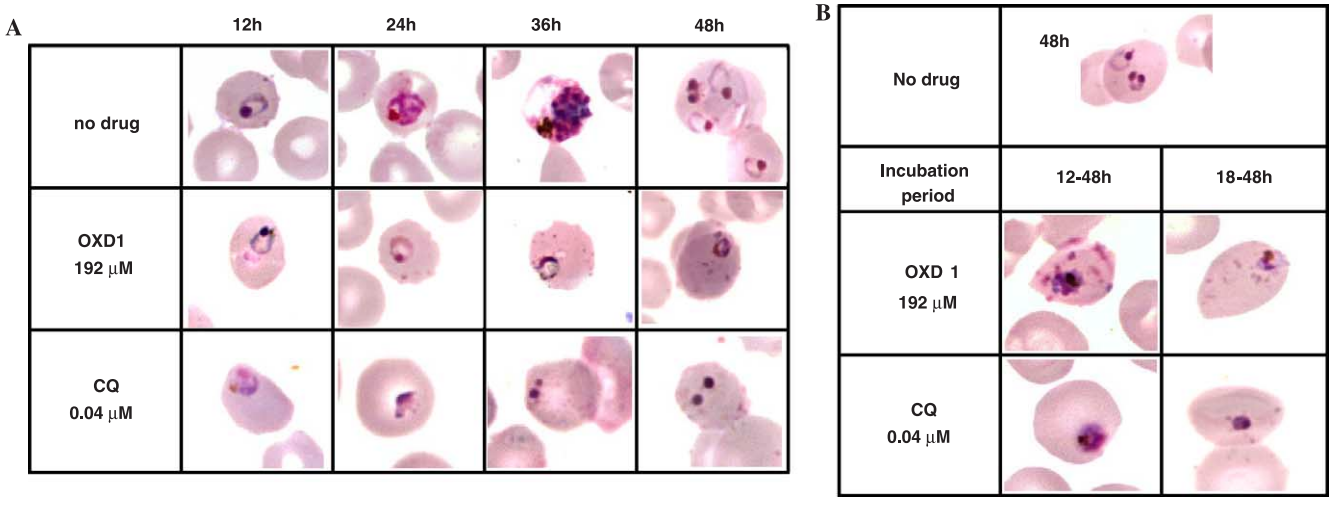

Fig. 5. Morphological changes to parasites observed after incubation with OXD1. Highly synchronous *P. falciparum* 3D7 cultures were exposed to 192 μM OXD1, 0.04 μM chloroquine or left untreated, at either the ring (A) or trophozoite stages (B). In (A) thin blood films were taken at the time points indicated during the 48 h cycle. In (B) the compounds were added at 12 or 18 h post-synchronization (ring-stage) and incubated until completion of the 48 h cycle at which point blood films were taken.

3.4. Effect of OXD1 on parasite growth over subsequent cycles

To determine whether parasites exposed to OXD1 at the ring or trophozoite stages are able to retain their potential for growth, parasite cultures were exposed to concentrations of OXD1 in excess of the IC_{99} value to ensure that the viability of the majority of parasites was affected. Parasite cultures were incubated for 48 or 96 h and then sub-cultured in the absence of the compound for up to 3 weeks. As shown in Fig. 6, parasites exposed to OXD1 at the ring stage for 48 h (Fig. 6A) or 96 h (Fig. 6B), reappeared at day 2 and at days 6–8, respectively, in the absence of OXD1. A more apparent delay was observed at the higher concentration of OXD1 (768 μM). Similar effects were observed with the lowest concentration of pyrimethamine (4 μM) but chloroquine treated parasites did not reappear after 96 h exposure. Incubation of the trophozoite stages (Figs. 6C and D) with OXD1 had a more pronounced effect, particularly after 96 h. By day 17 of culture in the absence of OXD1, no viable parasites were detected by microscopy at 768 μM whereas they began to reappear by day 14 at 384 μM. Parasites exposed to chloroquine at both concentrations and pyrimethamine at the highest concentration totally inhibited the reappearance of parasites following 96 h incubation with the drugs. In summary, compared to rings, a longer delay in the reappearance of parasites was observed when trophozoites were exposed to high concentrations of OXD1, confirming their increased susceptibility to this compound.

4. Discussion

In this study, we have characterized the stage specific anti-*P. falciparum* activity of the *Pf*LDH inhibitor OXD1. The compound inhibited the growth of a broad range of *P. falciparum* strains independently of their drug sensitivity profile suggesting a high degree of structural conservation of the *Pf*LDH active site between strains. Two different metabolic methods, [^{3}H]hypoxanthine incorporation and conversion of the vital dye hydroethidine into ethidium bromide, combined with microscopy, confirmed this anti-malarial effect. In contrast to gossypol derivatives that inhibit *P. falciparum* LDH by competitive binding to the NADH cofactor site and are cytotoxic (Gomez et al., 1997), OXD1 showed very low cytotoxicity to mammalian KB cells. This selective inhibition correlated with the preference for binding to the *Pf*LDH as compared to hLDH as we previously demonstrated (Cameron et al., 2004).

*Pf*LDH is one of the most abundant enzymes expressed by *P. falciparum* and is at high levels in the trophozoite stage (Vander Jagt et al., 1981; Basco et al., 1995). Recent analysis of the *P. falciparum* transcriptome using micro-array technology has shown that all glycolytic enzymes are upregulated at the early trophozoite stages during the asexual cycle, coinciding with the time of maximal metabolic activity by the parasite (Bozdech et al., 2003). We observed maximal *Pf*LDH mRNA expression and activity between 24 and 30 h of the cycle that correlated well with the increase in lactate

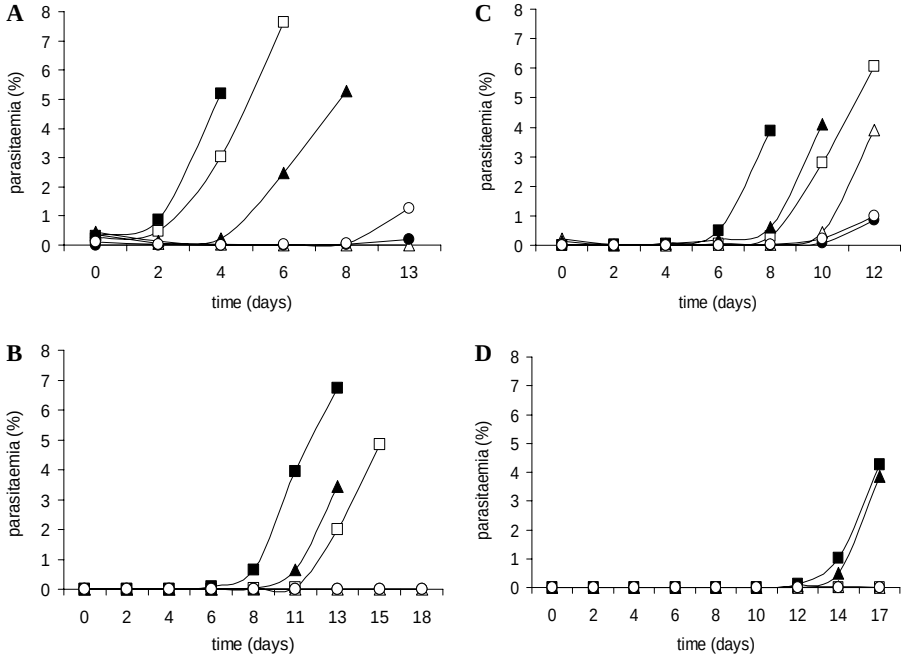

Fig. 6. Growth of *P. falciparum* over subsequent cycles. *P. falciparum* 3D7 was incubated for 48 or 96 h with OXD1. (A–D): IRBC were incubated with OXD1 (■, 384 μM;□, 768 μM), pyrimethamine (▲, 4 μM; △,40 μM) or chloroquine (●, 2 μM; ○, 0.4 μM) prior to washing and culturing in the absence of drug. Aliquots from each culture were removed and parasite viability assessed by microscopy at the times indicated. (A) Ring-stage parasites after incubation with the compounds for 48 h and (B) for 96 h. (C) Trophozoites incubated with the compounds for 48 h and (D) for 96 h.

levels previously reported at this stage (Pfaller et al., 1982; Vander Jagt et al., 1990).

The anti-malarial activity of OXD1 appeared to be stage-dependent as it exerted more pronounced inhibitory effects on the development of trophozoite than on ring stages. Although there was clear induction of pycnotic forms in a large proportion of parasites and a reduction in the parasitemia after OXD1 exposure, the recovery of parasites in the absence of OXD1, which was more rapid in the case of ring stages, suggests that targeting *Pf*LDH may have cytostatic rather than cytotoxic effects. These effects were cumulative with time (longer delay in recovery after 96 h compared to 48 h exposure) and are in agreement with the reported effects of the antifungal clotrimazole, another azole derivative that is not known to inhibit *Pf*LDH (Tiffert et al., 2000). Desferoxamine, an iron chelator, was also shown to have a cytotoxic effect at the trophozoite stage but a cytostatic effect at the ring stage (Whitehead and Peto, 1990). The less pronounced inhibitory effect that we observed after OXD1 treatment at the ring stage may be explained by their low energy requirements. Compared with the trophozoites, inhibition of *Pf*LDH at this stage may be less effective as a result of lower ATP requirements for maintaining parasite viability.

The high concentrations necessary to achieve an effect against trophozoites suggests that compound uptake may be a limiting factor. In preliminary drug uptake experiments, no evidence for preferential uptake of OXD1 within IRBC or URBC was found (data not shown) in comparison to chloroquine. It is possible that the stage-dependent differences observed with OXD1 arise through inhibition of other parasite processes, additional to pfLDH, in particular at the trophozoite stage. The identity of such putative targets remains unknown. Monocarboxylate transporters (MCTs) have been shown to be expressed at high levels at the trophozoite stage (Elliott et al., 2001) and the carboxylic acid anion of lactate has been shown to bind to the conserved active site of these transporters (Halestrap and Price, 1999). As OXD1 acts as a lactate competitor for pfLDH (Cameron et al., 2004), it can be speculated that OXD1 might also be accommodated by MCTs and may cause their inhibition.

In summary, these data strongly support the principle that specific inhibitors of *Pf*LDH can form effective non-toxic anti-malarial compounds. The high degree of structural conservation of the LDH active site between *P. falciparum*, *P. vivax*, *P. malariae*, and *P. ovale* (Brown et al., 2004) indicates that this class of azole compounds could have activity against the four species of human malarial parasites. Although it is accepted that glycolysis is the main source of energy in *Plasmodium*, *Pf*LDH gene knockout or RNA interference will confirm whether alternative stage-specific metabolic pathways are utilized in carbohydrate metabolism for ATP generation. Simultaneous inhibition of mitochondrial function and glycolysis and investigation by RNA micro-array analysis of the expression profile of other enzymes involved in energy production following inhibition of *Pf*LDH by OXD1 may add information in this respect. Nonetheless, this partial validation of *Pf*LDH as a drug target suggests that further optimization of azole derivatives is undoubtedly warranted in the search for new anti-malarial drugs with novel mechanisms of action.

Acknowledgments

This work was supported by Medicines for Malaria Venture, Grant MMV99/0006. We thank Dr. Kieran O'Dea for critical reading of the manuscript.

References

Azas, N., Laurencin, N., Delmas, F., Di, G.C., Gasquet, M., Laget, M., Timon-David, P., 2002. Synergistic in vitro antimalarial activity of plant extracts used as traditional herbal remedies in Mali. Parasitology Research 88, 165–171.

Basco, L.K., Marquet, F., Makler, M.M., Le Bras, J., 1995. *Plasmodium falciparum* and *Plasmodium vivax*: lactate dehydrogenase activity and its application for in vitro drug susceptibility assay. Experimental Parasitology 80, 260–271.

Blair, P.L., Witney, A., Haynes, J.D., Moch, J.K., Carucci, D.J., Adams, J.H., 2002. Transcripts of developmentally regulated *Plasmodium falciparum* genes quantified by real-time RT-PCR. Nucleic Acids Research 30, 2224–2231.

Bozdech, Z., Llinas, M., Pulliam, B.L., Wong, E.D., Zhu, J., DeRisi, J.L., 2003. The transcriptome of the intraerythrocytic developmental cycle of *Plasmodium falciparum*. Public Library of Science Biology 1, E5.

Brown, W.M., Yowell, C.A., Hoard, A., Vander Jagt, T.A., Hunsaker, L.A., Deck, L.M., Royer, R.E., Piper, R.C., Dame, J.B., Makler, M.T., Vander Jagt, D.L., 2004. Comparative structural analysis and kinetic properties of lactate dehydrogenases from the four species of human malarial parasites. Biochemistry 43, 6219–6229.

Cameron, A., Read, J., Tranter, R., Winter, V.J., Sessions, R.B., Brady, R.L., Vivas, L., Easton, A., Kendrick, H., Croft, S.L., Barros, D., Lavandera, J.L., Martin, J.J., Risco, F., Garcia-Ochoa, S., Gamo, F.J., Sanz, L., Leon, L., Ruiz, J.R., Gabarro, R., Mallo, A., Gomez de las Heras, F., 2004. Identification and activity of a series of azole-based compounds with lactate dehydrogenase-directed anti-malarial activity. Journal of Biological Chemistry 279, 31429–31439.

Desjardins, R.E., Canfield, C.J., Haynes, J.D., Chulay, J.D., 1979. Quantitative assessment of antimalarial activity in vitro by a semiautomated microdilution technique. Antimicrobial Agents and Chemotherapy 16, 710–718.

Dunn, C.R., Banfield, M.J., Barker, J.J., Higham, C.W., Moreton, K.M., Turgut-Balik, D., Brady, R.L., Holbrook, J.J., 1996. The structure of lactate dehydrogenase from *Plasmodium falciparum* reveals a new target for anti-malarial design. Nature Structural Biology 3, 912–915.

Elliott, J.L., Saliba, K.J., Kirk, K., 2001. Transport of lactate and pyruvate in the intraerythrocytic malaria parasite, *Plasmodium falciparum*. Biochemical Journal 355, 733–739.

Fleck, S.L., Birdsall, B., Babon, J., Dluzewski, A.R., Martin, S.R., Morgan, W.D., Angov, E., Kettleborough, C.A., Feeney, J., Blackman, M.J., Holder, A.A., 2003. Suramin and suramin analogues inhibit

merozoite surface protein-1 secondary processing and erythrocyte invasion by the malaria parasite *Plasmodium falciparum*. Journal of Biological Chemistry 278, 47670–47677.

Gomez, M.S., Piper, R.C., Hunsaker, L.A., Royer, R.E., Deck, L.M., Makler, M.T., Vander Jagt, D.L., 1997. Substrate and cofactor specificity and selective inhibition of lactate dehydrogenase from the malarial parasite *P. falciparum*. Molecular and Biochemical Parasitology 90, 235–246.

Guerin, P.J., Olliaro, P., Nosten, F., Druilhe, P., Laxminarayan, R., Binka, F., Kilama, W.L., Ford, N., White, N.J., 2002. Malaria: current status of control, diagnosis, treatment, and a proposed agenda for research and development. Lancet Infectious Diseases 2, 564–573.

Halestrap, A.P., Price, N.T., 1999. The proton-linked monocarboxylate transporter (MCT) family: structure, function and regulation. Biochemical Journal 343 (Pt 2), 281–299.

Homewood, C.A., Neame, K.D., 1983. Conversion of glucose of lactate by intraerythrocytic *Plasmodium berghei*. Annals of Tropical Medicine and Parasitology 77, 127–129.

Jensen, M.D., Conley, M., Helstowski, L.D., 1983. Culture of *Plasmodium falciparum*: the role of pH, glucose, and lactate. Journal of Parasitology 69, 1060–1067.

Lang-Unnasch, N., Murphy, A.D., 1998. Metabolic changes of the malaria parasite during the transition from the human to the mosquito host. Annual Review of Microbiology 52, 561–590.

Makler, M.T., Ries, J.M., Williams, J.A., Bancroft, J.E., Piper, R.C., Gibbins, B.L., Hinrichs, D.J., 1993. Parasite lactate dehydrogenase as an assay for *Plasmodium falciparum* drug sensitivity. American Journal of Tropical Medicine and Hygiene 48, 739–741.

Olliaro, P.L., Taylor, W.R., 2003. Antimalarial compounds: from bench to bedside. Journal of Experimental Biology 206, 3753–3759.

Pfaller, M.A., Krogstad, D.J., Parquette, A.R., Nguyen-Dinh, P., 1982. *Plasmodium falciparum*: stage-specific lactate production in synchronized cultures. Experimental Parasitology 54, 391–396.

Ridley, R.G., 2003. Malaria: to kill a parasite. Nature 424, 887–889.

Roth Jr., E., 1990. *Plasmodium falciparum* carbohydrate metabolism: a connection between host cell and parasite. Blood Cells 16, 453–460.

Tiffert, T., Ginsburg, H., Krugliak, M., Elford, B.C., Lew, V.L., 2000. Potent antimalarial activity of clotrimazole in in vitro cultures of *Plasmodium falciparum*. Proceedings of the National Academy of Sciences of the United States of America 97, 331–336.

Trager, W., Jensen, J.B., 1976. Human malaria parasites in continuous culture. Science 193, 673–675.

Turgut-Balik, D., Shoemark, D.K., Sessions, R.B., Moreton, K.M., Holbrook, J.J., 2001. Mutagenic exploration of the active site of lactate dehydrogenase from *Plasmodium falciparum*. Biotechnology Letters 23, 923–927.

Vander Jagt, D.L., Hunsaker, L.A., Campos, N.M., Baack, B.R., 1990. D-lactate production in erythrocytes infected with *Plasmodium falciparum*. Molecular and Biochemical Parasitology 42, 277–284.

Vander Jagt, D.L., Hunsaker, L.A., Heidrich, J.E., 1981. Partial purification and characterization of lactate dehydrogenase from *Plasmodium falciparum*. Molecular and Biochemical Parasitology 4, 255–264.

Whitehead, S., Peto, T.E., 1990. Stage-dependent effect of deferoxamine on growth of *Plasmodium falciparum* in vitro. Blood 76, 1250–1255.

Wyatt, C.R., Goff, W., Davis, W.C., 1991. A flow cytometric method for assessing viability of intraerythrocytic hemoparasites. Journal of Immunological Methods 140, 23–30.